

## SIMULTANEOUS DIELECTRIC ANALYSIS-DIFFERENTIAL THERMAL ANALYSIS OF SOLID MATERIALS\*

KRISHNAN RAJESHWAR, RICHARD N. NOTTENBURG AND JOEL B. DUBOW

*Electrical Engineering Department, Colorado State University, Fort Collins, Colorado 80523 (U.S.A.)*

### ABSTRACT

A novel technique has been developed wherein dielectric analysis (DA) and differential thermal analysis (DTA) are performed simultaneously on a single test material. The speed of data acquisition and the range of frequencies and temperatures that can be investigated in a single experiment are far beyond the capabilities of conventional techniques. The frequency range for dielectric measurements can be pre-selected in fixed steps over the range  $1-10^7$  Hz. DA and DTA measurements are carried out over the temperature range 25-800°C. The present technique, which features extensive automation in data acquisition and processing, is illustrated by preliminary measurements on Colorado Green River oil shale. The results indicate that a combined use of DA and DTA techniques yields useful information for elucidation of thermal decomposition and phase transformation mechanisms.

### INTRODUCTION

Sample heterogeneity and compositional variations inherent in naturally occurring materials like shales and minerals pose special problems in studying their physico-chemical behavior and lead to difficulties in the correlation of results obtained from one experimental technique with those acquired from another. It is, therefore, desirable to perform simultaneous measurements on such materials. Very often a definite advantage is gained by the more complete information derived therein by such an approach; the utility and inadequacy of the measurement of one property of the material is complemented and compensated by a simultaneous measurement of another property of the same sample. The thermal and electrical properties of a material are extremely important in the characterization of its physico-chemical behavior. Two techniques which are extensively employed for the study of these properties are differential thermal analysis (DTA) and dielectric analysis (DA). This paper describes the realization and utilization of an apparatus which features simultaneous application of the two techniques on a single specimen. The apparatus

\* Presented at the 7th North American Thermal Analysis Society Conference, St. Louis, Missouri, September 25-28, 1977.

features a novel method of measurement of the dielectric properties as a function of both temperature and frequency; the measurement speed, amount of data, and the range of frequencies and temperatures that can be spanned in a single experiment with this method are far beyond the capabilities of conventional bridge techniques. The technique of simultaneous dielectric and differential thermal analysis is illustrated by preliminary measurements on samples of Colorado Green River oil shale.

Green River oil shale has been the subject of several investigations by thermal analysis techniques<sup>1-4</sup>. Simultaneous application of DTA with thermogravimetric analysis (TGA) and evolved gas analysis (EGA) has been carried out by Smith and Johnson<sup>4</sup> with a view to studying the decomposition of the organic and mineral matter in oil shale. However, oil shale is a complex, heterogeneous material; it exhibits temperature-dependent behavior which is difficult to characterize using conventional thermal analysis techniques. For example, Tisot<sup>5, 6</sup> reports a transition below the retorting temperature during which oil shale at first loses, and then regains structural strength. Significant variations in other properties like the thermal conductivity, expansion coefficient, d.c. electrical conductivity and a.c. electrical impedance have also been observed by DuBow et al.<sup>7, 8</sup> at temperatures corresponding to the decomposition of the organic matter in oil shale. Therefore, with this and other evidence becoming available in the past few years, it has become increasingly apparent that there is a need for other techniques in addition to DTA and TGA, in order to fully characterize thermal decomposition and phase transformation mechanisms, especially in naturally occurring materials.

One technique which has been rather neglected by thermal analysts is that of dielectric analysis. This is somewhat surprising, especially when one considers the fact that the ability of this technique to "see" things on a microscopic level offers a number of advantages in the interpretation of DTA and other thermal analysis data. For example, changes in symmetry arising from a phase transformation, possibly, but not necessarily, brought about by a decomposition process, may bring about a change in the rotational freedom of a molecule or ion with a resultant change in the polarizability and hence the dielectric properties. Correlation of such information with the thermal data from DTA or TGA could be valuable in formulating an overall mechanism for the reaction of interest.

In the light of the above, an apparatus which can perform simultaneous DA and DTA on a single specimen, would be extremely useful, particularly in problems related to the study of natural materials. Accordingly, this investigation was undertaken with a view to (a) developing a suitable apparatus for the simultaneous application of DA and DTA, (b) illustrating the utility of the technique by measurements on Colorado Green River oil shale, and (c) correlating the thermal and dielectric behavior of these oil shales.

## EXPERIMENTAL

A schematic view of the apparatus for DA-DTA is shown in Fig. 1.

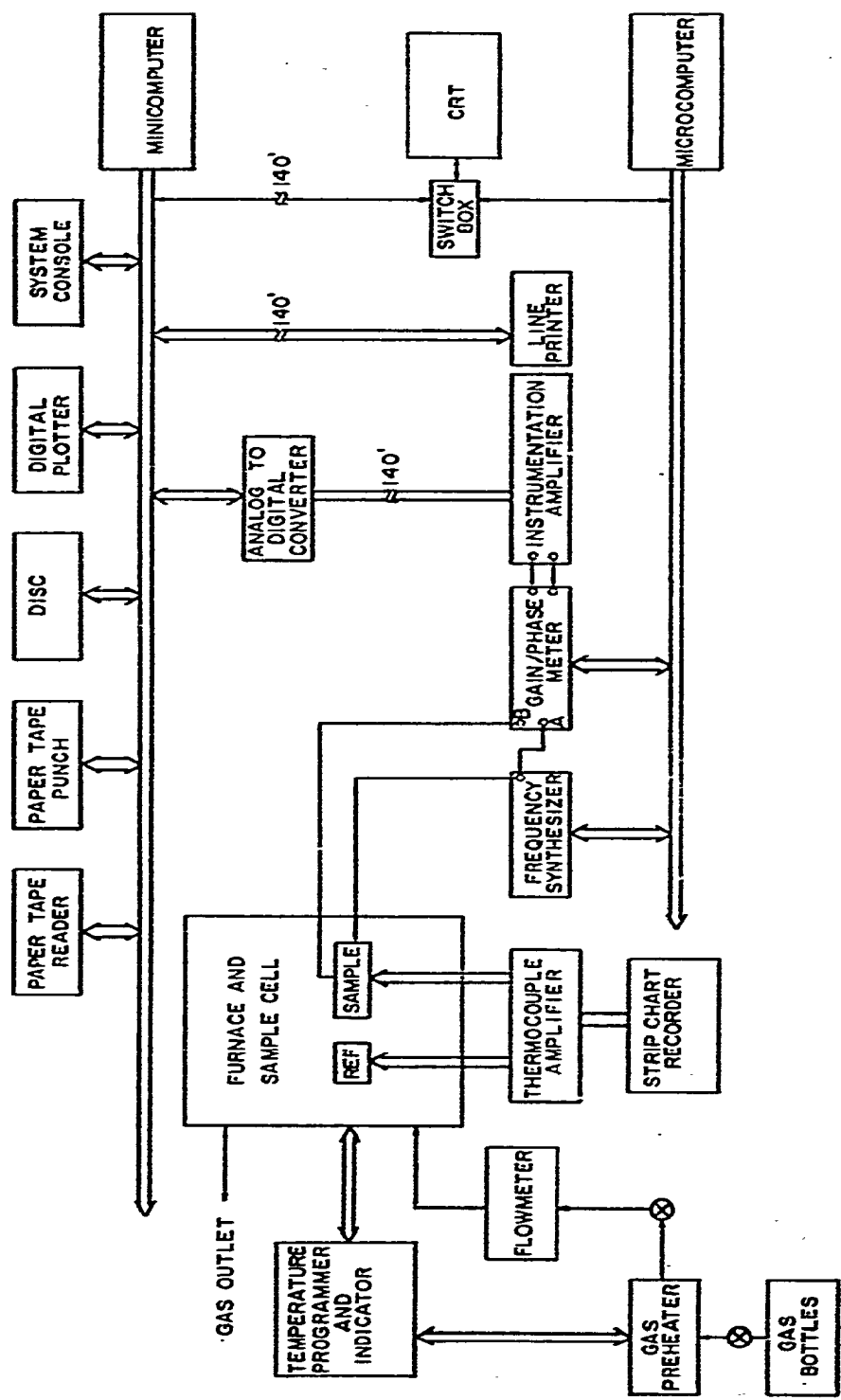


Fig. 1. A schematic of the DA-DTA system.

### Apparatus

The main components of the experimental arrangement for simultaneous DA-DTA employed in the present investigation are detailed below.

**Furnace.** The furnace used in the present investigation is a vertical type with a tubular heating chamber and is shown in Fig. 2. It uses Kanthal heater elements wound on two semicircular ceramic cores. A, the heater wires, are insulated from each other and from other metallic parts, by a thick coating of alundum cement (Fisher Scientific Co.). The two heating cores are bolted onto a circular asbestos sheets, B (1/2 in., 10 in. diameter) so as to form a cylindrical heating chamber 6 in. high and 6 in. diameter. The space between the heating core and the inner steel casing, C, is packed with low-density insulation material composed mainly of vermiculite. The inner circular casing (19.5 in. o.d.) is made of 1/4 in.-thick stainless steel; it is fixed to the heating core by tight-fitting asbestos sheets, D and B, at the top and at the bottom (see Fig. 2). The electrical connections for the furnace are drawn out through the bottom asbestos sheet, B, through ceramic insulators. The space between the asbestos strip and the bottom plate of the inner stainless steel casing is again packed with asbestos powder and vermiculite insulation. The control thermocouple, E, is located in close proximity to the heater winding for efficient temperature control. The outer shield for the furnace, F, (height 12 in., diameter 12.5 in.) is made of aluminum sheet 1.125 in. thick. The column of air separating the outer shield from the inner stainless steel casing provides good thermal insulation for the furnace. Holes are drilled in the aluminum plate, G, at the bottom and in the lower asbestos sheet of the furnace for electrode connections and gas outlet. The large mass of insulation surrounding the heater chamber is effective in providing a good thermal stability. Convection cooling at the top end of the hot zone and "end-effects" are minimized by the asbestos insulation at the top, the column of air above the hot zone and by the aluminum sheet, H, at the top. The maximum power rating of the furnace is 2.4 kW and the unit operates on a 115 V a.c. supply.

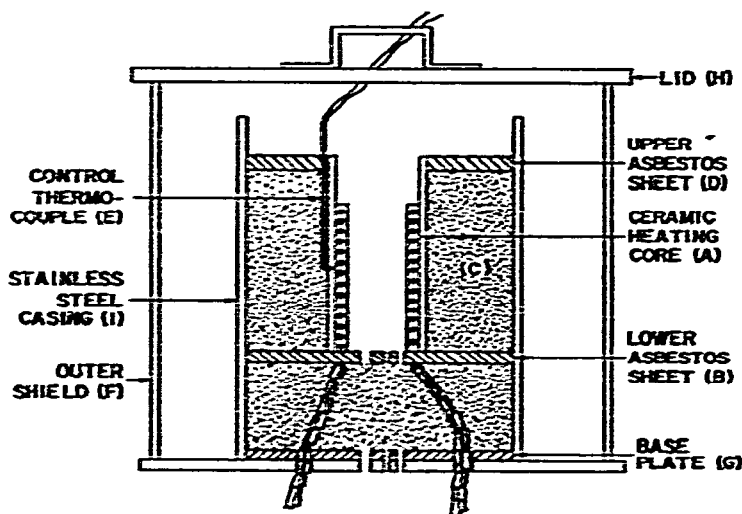


Fig. 2. A cross-sectional view of the furnace.

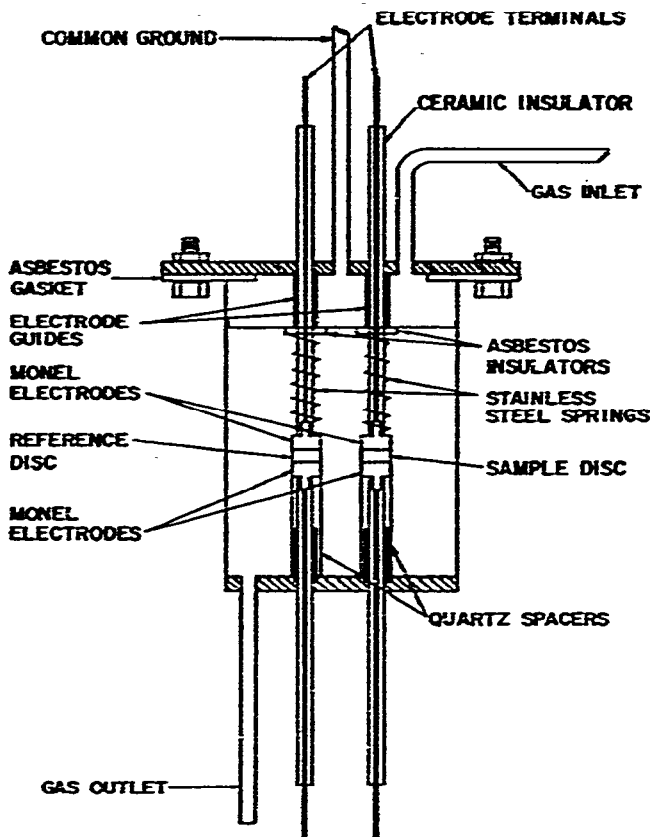


Fig. 3. Sample cell for DA-DTA.

*Sample vessel.* The sample vessel used in the study is made of stainless steel and is illustrated in Fig. 3. The main factors that have been taken into consideration in the design of the sample vessel are

- (a) to allow a range of sample sizes to be used
- (b) to permit dynamic gas atmospheres to be employed and effluent gases analyzed
- (c) to allow static controlled atmospheric operation
- (d) to permit sample supports to be interchanged to accommodate different types of samples
- (e) to have the temperature to be recorded chosen from one of the following points: sample, reference or the sample-holder wall
- (f) to support the sample in such a manner that both DTA and dielectric measurements can be made at the same time and
- (g) to facilitate convenient handling and maintenance of samples, electrodes, thermocouples and other connections.

The dimensions of the sample vessel are such that it fits exactly inside the heating chamber of the furnace. The outlet for the sweep gas and for the exhaust gases, consisting of a stainless steel tube (length 10 in., o.d. 1/4 in., i.d., 1/16 in.) welded to

the bottom of the vessel, passes through holes in the lower asbestos sheet, B, and the bottom plate, G, of the furnace and fits inside a copper tube connected to the exhaust manifold. Swagelok fittings are provided at the bottom plate of the vessel and also on the lid for guiding the electrodes. The electrode leads consist of 26-gauge silver wire held in place inside ceramic insulation tubes (1/4 in. o.d., Coors Porcelain Co., Golden, Colorado) by Saureisen Insu-late Adhesive Cement. The leads are connected to Monel electrodes (1/2 in. diameter, 1/4 in. thick) by suitable threading. The arrangement of the samples and reference discs inside the vessel is such that the Monel plates with the ceramic support tubes serve both for holding the specimens in place and also as electrodes. The lower support tubes are held in place by quartz spacers (1/2 in. diameter) which are held in place over the electrode guides on the base plate of the sample vessel. The lower support tubes fitting inside the spacer tubes are inserted into the guide fittings and out through the bottom plate, G, of the furnace. The support tubes at the top are passed through a thin stainless steel strip bolted to the sides of the sample vessel. Compression springs made of high-temperature alloy steel (AAAA Specialties, Denver, Colorado) are slipped over the support tubes at the top and are held in place by the stainless steel strip. The springs exert a force downwards on the Monel plates and hold the sample and reference discs in place. The springs are electrically insulated from the electrodes by asbestos O-rings.

The lid for the sample vessel consists of a circular stainless steel plate with holes drilled in it for electrical and thermocouple connections. The lid can be bolted tightly to the sample vessel and an asbestos gasket between the lid and the vessel prevents leakage of sweep gas and reaction gases during operation. The inlet tube for the sweep gas consists of a stainless steel tube welded onto the lid.

In a typical operation, the sample vessel is inserted in place inside the heating chamber of the furnace. Electrode connections are made at the bottom and the gas outlet tube is connected to the exhaust manifold. The sample and reference discs are slipped in between the Monel plates. Special care is taken to see that the sample and the electrodes are properly aligned. The thermocouple connections from the sample and reference discs are taken out through the holes in the lid. The upper support tubes with the electrode leads are inserted through the holes in the lid which is then bolted to the vessel. Connection of the sweep gas supply to the inlet tube and hook-up of the thermal and electrical leads to the appropriate panels complete the cycle of operation. Loading the sample and reference discs and preparing the unit for operation typically takes about fifteen minutes.

The electrodes with the support tubes can be removed after an experiment and the sample vessel cleaned by removing the stainless steel strip at the top. All parts of the sample vessel are grounded to avoid electrical noise and problems due to stray current paths. The stainless steel vessel also serves as an effective shield for 60 Hz and other stray electromagnetic radiation. The vessel is electrically insulated from the heater elements by alundum cement and by a thick asbestos gasket at the top.

*Temperature controller and programmer.* The temperature controller and programmer used in the present investigation is a modified Deltatherm III (Technical

Equipment Corporation, Denver, Colorado) unit. Extensive modifications have been made on the original programmer to (1) enable it to operate on a simultaneous DA-DTA mode; (2) drive the furnace described above; and (3) provide additional power required by the use of a larger load.

The programmer is capable of heating rates ranging from 0.5–10°C/min. However, the power requirements of the DA-DTA furnace are such that heating rates higher than 5°C/min seldom give good linearity and reproducibility. This, in any case, is not critical since high heating rates cannot be employed in DA-DTA. The time required for the swept frequency dielectric measurement at a particular temperature sets a natural limit for the heating rate that can be employed.

Most of the experiments in the present investigation were carried out at a heating rate of 2.5°C/min. The total amplification of the amplifier-recorder combination for the differential thermocouple output is adjustable in fixed steps from 0.05 to 10°C/in.

*Gas pre-heating and flowing atmosphere operation.* The problems of oxidation and combustion encountered in studies of naturally occurring fuels and similar materials necessitate efficient control of the atmospheres prevailing over the samples. The exothermic reactions in air arising from oxidation and combustion of such materials dominate the thermal record, precluding the discovery of any additional information<sup>9</sup>. Atmosphere control requires prompt removal of product gases from the entire sample and their replacement by the selected gas. If the products are not removed promptly, a non-reproducible self-generated atmosphere results<sup>10-13</sup>. The disastrous consequences this has in studies on oil shale and related materials have been pointed out in previous studies<sup>14, 15</sup>.

The schematic for the flowing gas control used in the present investigation is shown in Fig. 4. The gas preheating arrangement is designed primarily for very high flow rates where problems due to irreproducible heating rates and non-uniform temperature gradients are inherent. The gas heating system is shown in Fig. 4A and the associated electronics in Fig. 4B. The gas from the main supply line enters an inlet thin-walled tube made of stainless steel. The inlet tube is fitted to the bottom of a ceramic tube (1 in. diameter) packed with 1/4 in. diameter stainless steel ball bearings. The outlet tube, also made of stainless steel, is connected to a flow meter through a valve. The ceramic tube is heated by a small resistance heater (Technical Equipment Corporation, Denver, Colorado) which is electronically coupled to the main furnace. The ceramic tube and the stainless steel ball bearings provide good heat transfer between the hot solids and the incoming gas and also a long pathlength so that the gas coming out is essentially at the same temperature as the heater system. The control thermocouple for the gas-preheating system is located between the ceramic tube and the heater winding.

A block diagram of the circuit for the preheating unit is shown in Fig. 4B. The unit essentially consists of a proportional controller driven by an error amplifier. The controller tracks the temperature of the main furnace and accordingly supplies the required amount of power to the gas heater. The error amplifier has a gain of  $10^4$  and

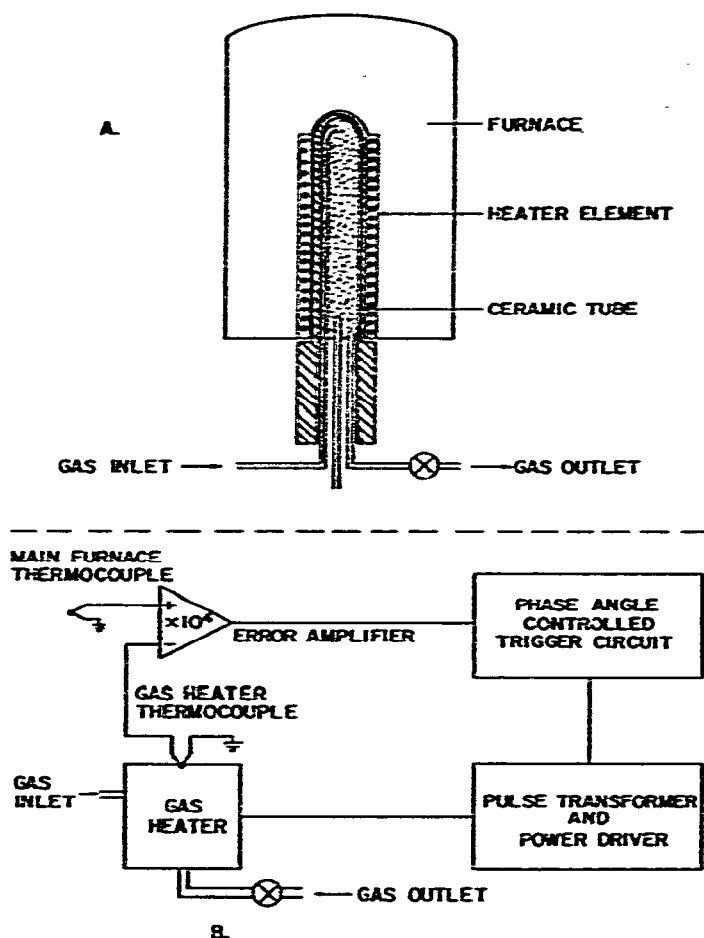


Fig. 4. Schematic of gas pre-heating arrangement. A, Flow tube. B, Control circuit.

an error signal of 1 V drives on 95% of the maximum power to the heater. At the highest flow rate employed in the experiment ( $\sim 150$  ml/min), the difference between the furnace temperature and the gas heater temperature is less than  $1^\circ\text{C}$ .

*Electrical impedance measurement apparatus.* A Hewlett-Packard Model 3320B frequency synthesizer provides the sinusoidal source used in the present investigation. Remote control is accomplished by 8080 control of the BCD data lines.

Measurement of the changes in the amplitude and phase of the sinusoidal signal, after passage through the test material, is carried out by a Hewlett-Packard Model 3575 A Gain-Phase Meter. The frequency response of this instrument extends from 1 Hz to 13 MHz in four overlapping frequency ranges. Remote control operation and automatic acquisition of gain-phase values have been facilitated with the aid of an 8080 microprocessor and HP 2100 minicomputer. Details of the operation and the control programs are discussed elsewhere<sup>16</sup>.

The impedance measurement for dielectric analysis is based upon the determination the phase shift and attenuation (gain) of a sinusoidal signal as it is passed



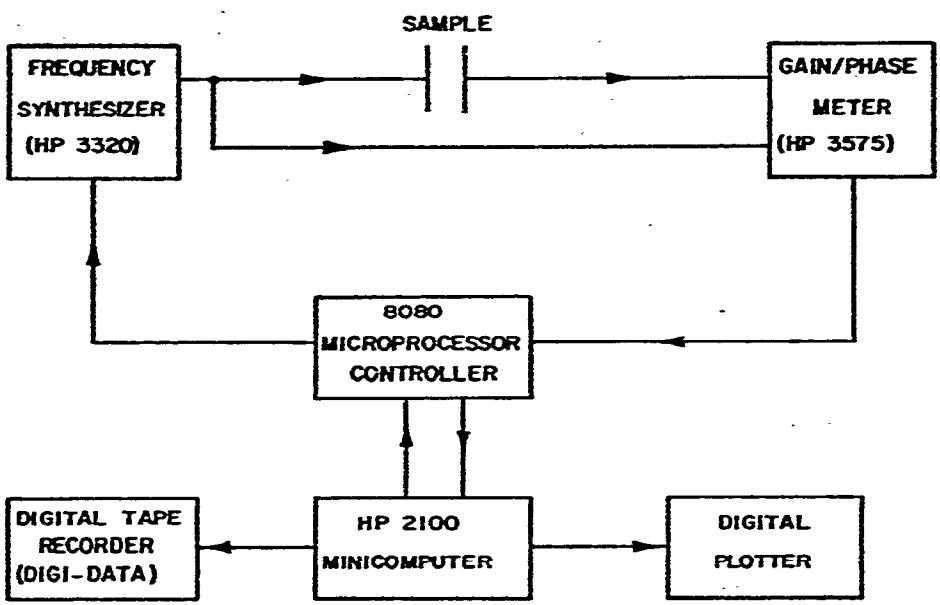
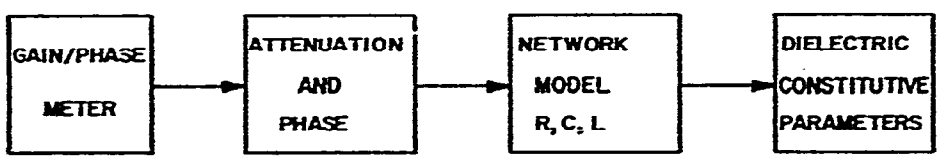


Fig. 5. Data flow for dielectric analysis.



through the sample. Using the attenuation and phase shift data, the element values of an equivalent circuit consisting of passive electrical components are determined. From these element values, the equivalent dielectric constant  $\epsilon'$ , loss tangent  $\tan \delta$ , and conductivity  $\sigma$  are determined. Figure 5 shows the data analysis path.

After the attenuation and phase angle at a given frequency are determined, these data are transmitted to a HP 2100 minicomputer through an HP 8080 microprocessor system. Following this data transmission, the microprocessor signals the sinusoidal signal source to increase the frequency by a preselected increment.

*Data acquisition and processing.* Data acquisition for dielectric analysis is completely automated; programs have been developed for conversion of raw experimental data to parameters that can be directly correlated with work previously reported in the literature. The parameters,  $\epsilon'$ ,  $\epsilon''$ ,  $\tan \delta$  and  $\sigma$  as a function of frequency

( $f$ ) and temperature are either printed out on a Centronics Model 503 Printer (Centronics Data Computer Corporation, Hudson, New Hampshire) or plotted on a Model 7210A Hewlett-Packard Digital Plotter.

The DTA curves are recorded either on an omnigraphic Series 2-3000 two-pen strip-chart recorder (Houston Instruments, Bellaire, Texas) or on a Hewlett-Packard Model 7004B X-Y Recorder. The strip-chart recorder has chart speeds ranging from 0.05 to 20 in./min. DTA curves are recorded as a function of time on the strip-chart recorder, one channel being chosen for  $\Delta T$  and the other for  $T_{ref}$ . This mode of recording is decidedly superior to  $\Delta T$  vs.  $T_{ref}$  curves<sup>17</sup>.

### *Sample preparation*

The technique of simultaneous DA-DTA developed in the course of this investigation is illustrated by preliminary measurements on Colorado Green River oil shale.

The samples of oil shale for the measurements have been gathered from the Paraho Mine, just west of Rifle, Colorado. This mine is located in the Piceance Creek Basin in the Mahogany Zone<sup>18</sup>. The selection of samples has been designed to cover a wide range of grades; care is also taken to select samples which are crack-free. The rock specimens are first cored to 7/8 in. diameter cylindrical sections using a drill press. The cylindrical sections are then cut to 1/4 in.-thick discs using an automatic-feed diamond saw (Raytech Corporation, 10 in. type L-105).

### *Procedure*

The sample and reference discs are first loaded in the sample vessel. Thermocouple connections are then made, care being taken to insure that the wires are properly in place in the discs. The electrodes are then connected to the frequency synthesizer and gain-phase meter through coaxial cables. The gas supply is turned on, and the valve to the flowmeter is adjusted to obtain a preselected flow rate of the sweep gas. The system is thoroughly flushed with the inert gas for about twenty minutes. The heating rate on the programmer is then set at the desired level and the recorder-amplifier ranges are set for the DTA scan. The upper temperature limit of the scan is chosen and the system is switched on. While the various instruments are warming up, the computer is readied for operation and the programs are loaded into the computer from a CRT terminal (Learseigler LS 13) for the swept-frequency gain-phase measurements. The number of frequency points to be scanned in each decade is preselected and loaded into the 8080 microcomputer. The settling times at each frequency are also predetermined. After the heating of the sample and reference is initiated, a complete frequency spectrum of the gain-phase values is scanned at various temperatures. The scan rate can be adjusted; a typical scan rate is 3 min from 1 to  $10^7$  Hz. The temperature at the start and end of each scan is also recorded. In order to minimize rapid changes in temperature during a gain-phase measurement, it is important to employ low heating rates for the DTA measurements. Very low heating rates, of course, give rise to DTA peaks high in resolution but weak in intensity.

A compromise is, therefore, sought between the minimum sensitivity that can be obtained for the differential temperature and the highest heating rate that can be employed for DA measurements. A heating rate of  $2.5^{\circ}\text{C}/\text{min}$  has been found to give reasonably good results for simultaneous DA-DTA. An average of about twenty-five temperatures are selected for gain-phase measurements for each DA-DTA experiment; the number and frequency of scans depends on the thermal behavior of the test material as evidenced by the simultaneous DTA data and also by the rate of change of the gain-phase values that is observed as a function of temperature. The operator can examine the gain-phase data being processed by displaying the results on a graphic terminal or other output device. The analog output of the gain-phase meter can also be recorded simultaneously on an X-Y or a strip-chart recorder as a function of frequency. Usually, the gain-phase values are monitored more frequently in a preliminary scan of an unknown test material. A particular temperature range of interest can then be selected from the DTA curves, for a subsequent detailed investigation. DTA in an isothermal mode as a function of time is also another interesting possibility. The variation in the parameters as a function of time, during the course of a thermal decomposition or phase transformation, can thus be monitored.

Gain-phase results from each scan are recorded on a moving head disc. Data is organized into files in computer memory for reduction by automatic analysis programs.

## RESULTS AND DISCUSSION

Figures 6 and 7 show representative DTA curves on Green River oil shale obtained with the apparatus described above. These curves were obtained simultaneously with the DA carried out on the same samples (see later). The thermal decomposition of the organic matter in the shale is seen to be endothermic in nature and takes place in the range  $400\text{--}500^{\circ}\text{C}$ . It must be noted that the decomposition temperatures are markedly dependent on the source and type of oil shale. Considerable variations have been observed in the temperatures corresponding to the decomposition of the organic matter, the peak temperatures in some cases as low as  $350^{\circ}\text{C}$ . The thermal and depositional history of the sample is, therefore, of extreme importance for their useful characterization by DTA. The splitting of the endothermic peaks in Figs. 6 and 7 seems to indicate that the thermal decomposition of the organic matter in the shale is a multistep process. The small peak at  $352^{\circ}\text{C}$  possibly arises from the thermal decomposition of analcite, initially present in the shale. This assignment is consistent with the results of previous work on the thermal characteristics of analcite<sup>19</sup>. None of the oil shale samples examined in the present work shows significant amounts of nahcolite, as evidenced by the absence of peaks in the range  $150\text{--}200^{\circ}\text{C}$ <sup>20</sup>.

Figures 8 and 9 depict the behavior of the dielectric constant of a 66.7 gal per ton (gpt) shale as a function of temperature and frequency. Similar behavior is observed for other grades. The dielectric constant is seen to decrease from a relatively high value at low frequencies to a lower value at high frequencies. In addition, the dielectric constant is seen to initially decrease with increasing temperature. However,

SAMPLE: OIL SHALE  
 GRADE: 40 GALLONS/TON  
 REFERENCE: ALUMINA  
 ATMOSPHERE: FLOWING N<sub>2</sub>  
 HEATING RATE: 2.5°C/min  
 THERMOCOUPLES: CHROMEL/ALUMEL, TYPE K

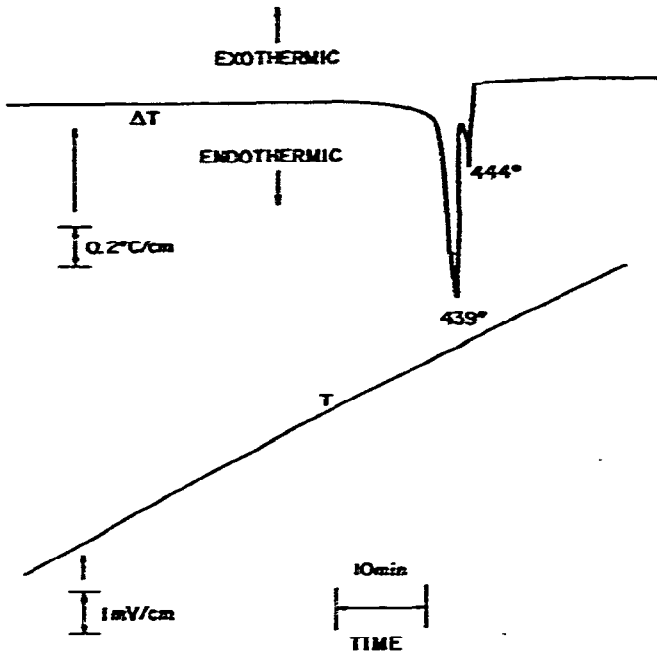


Fig. 6. Time-based DTA record of Green River oil shale.

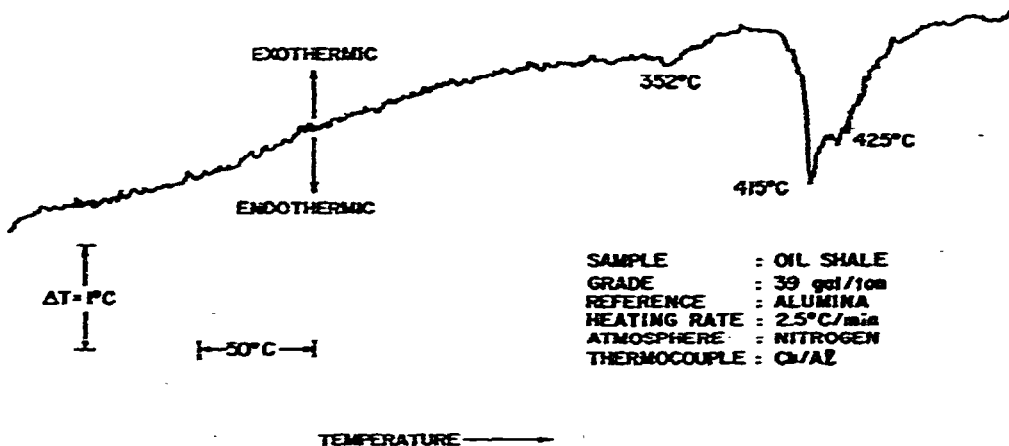


Fig. 7. DTA curve ( $\Delta T$  vs.  $T_{ref}$ ) for a 39 gallons/ton oil shale sample.

at about 250°C, the dielectric constant is seen to begin increasing again, particularly at lower frequencies. At temperatures where significant amounts of organic decomposition occur, the low frequency dielectric constant attains values approaching the low temperature values. However, the falloff with frequency is more rapid. The origins of this effect are as yet not well understood. Pore pressure effects and capillary

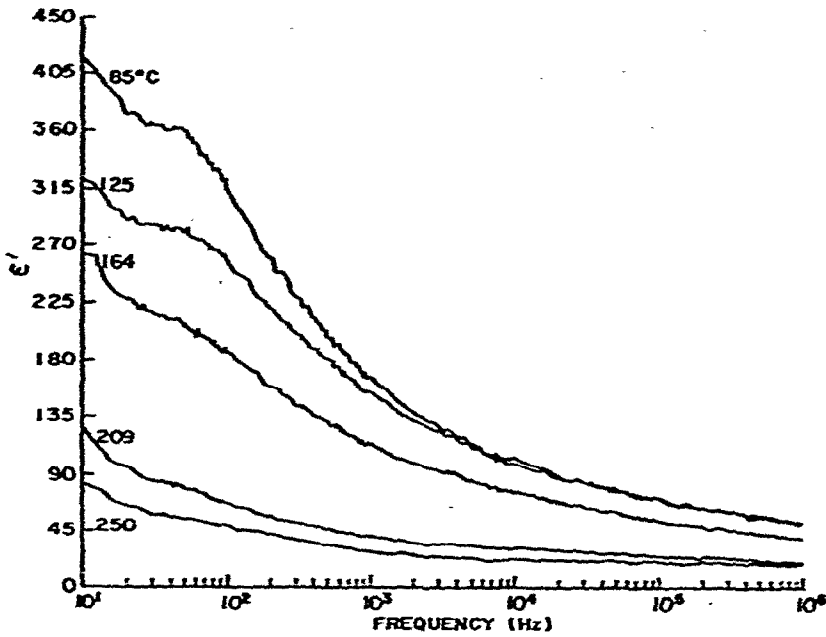


Fig. 8. Low-temperature dielectric constant of Green River oil shale as a function of frequency.

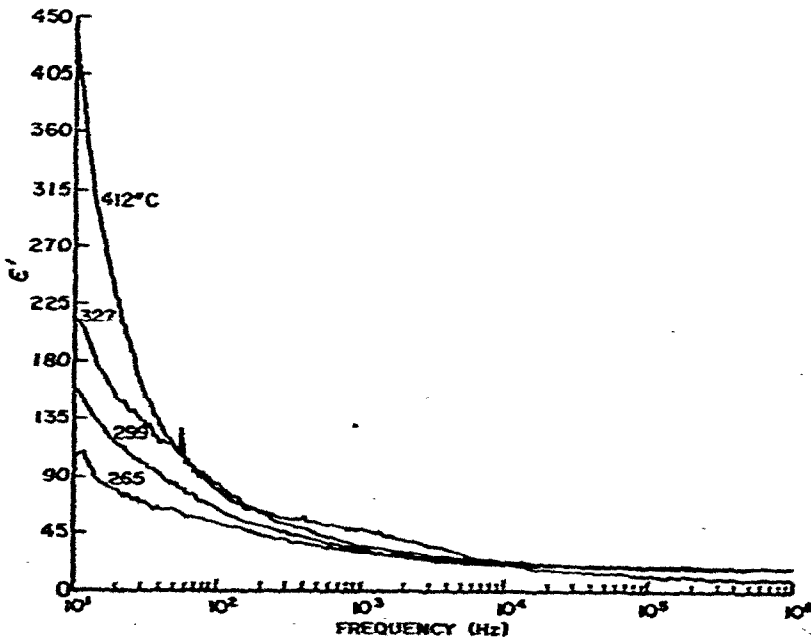


Fig. 9. High-temperature dielectric constant of Green River oil shale as a function of frequency.

water in the shale could possibly play a role in this effect. This possibility is indicated by the shift in the baseline slope on the DTA at about 250°C.

Typical data showing the variation of the dielectric parameters with frequency are shown in Table 1 for a 37 gpt oil shale sample. The dielectric constant  $\epsilon'$  shows the frequency dependence characteristic of other water-bearing sedimentary rocks and

TABLE 1

DIELECTRIC ANALYSIS OF GREEN RIVER OIL SHALE (37 gpt)

Frequency (Hz)	Resistivity (ohms-cm)	Capacitance (farad)	$\epsilon'$	$\epsilon''$	$\tan \delta$	a.c. Conductivity (mho $\text{cm}^{-1}$ )
10	$0.100 \times 10^{11}$	$0.161 \times 10^{-10}$	18.54	1.831	0.098	$0.102 \times 10^{-10}$
50	$0.442 \times 10^{10}$	$0.164 \times 10^{-10}$	18.90	0.829	0.043	$0.231 \times 10^{-10}$
100	$0.236 \times 10^{10}$	$0.164 \times 10^{-10}$	18.91	0.776	0.041	$0.432 \times 10^{-10}$
1000	$0.480 \times 10^9$	$0.150 \times 10^{-10}$	17.21	0.382	0.022	$0.212 \times 10^{-9}$
4000	$0.369 \times 10^8$	$0.142 \times 10^{-10}$	16.28	1.240	0.076	$0.276 \times 10^{-8}$
10,000	$0.963 \times 10^7$	$0.134 \times 10^{-10}$	15.35	1.901	0.124	$0.106 \times 10^{-7}$
52,000	$0.113 \times 10^7$	$0.108 \times 10^{-10}$	12.39	3.113	0.251	$0.102 \times 10^{-6}$
94,000	$0.808 \times 10^5$	$0.552 \times 10^{-11}$	6.35	2.410	0.380	$0.126 \times 10^{-5}$

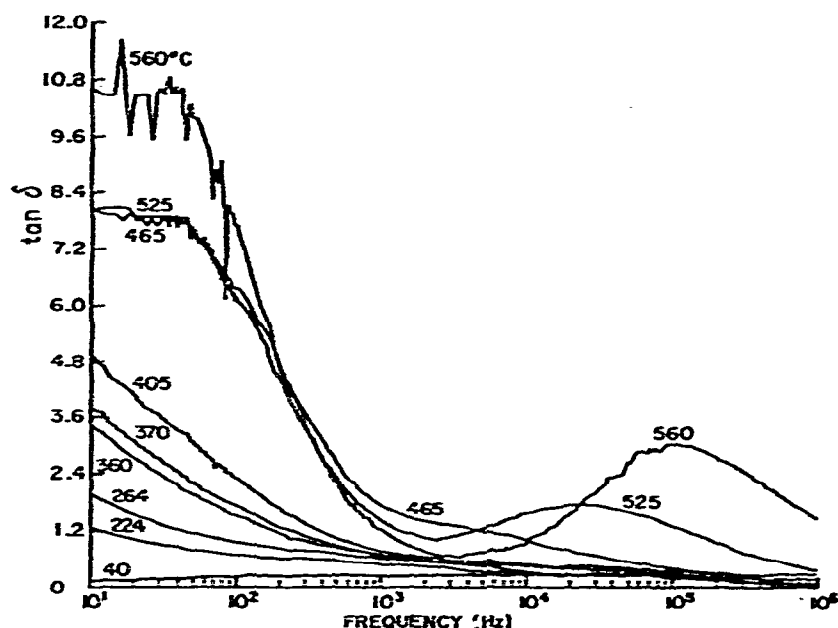


Fig. 10. Temperature-dependent loss-tangent versus frequency for a 26 gallons/ton oil shale.

minerals<sup>21</sup>, a sharp decrease in dielectric constant at low frequencies and a very gradual decrease with increasing frequency at higher frequency values. The high values of the low frequency dielectric constant found for the oil shale samples may be explained in terms of the Maxwell-Wagner theory for interfacial polarization<sup>22</sup>. The presence of semiconducting clay particles which give rise to a membrane effect, might also account for the large values of dielectric constant<sup>23</sup>. The data shown in Table 1 also reveal a sharp increase in the a.c. conductivity with increasing frequency. This behavior is consistent with previously published work on the electrical properties of limestone, marl and dolomite<sup>21</sup>, which show that the lower the water content and/or

the higher the resistivity of the material, the greater is the decrease in the resistivity with increasing frequency. The water content of oil shale is variable; however, it seldom exceeds 6–10%, which is well within the limits observed for sedimentary rocks which exhibit similar dielectric behavior.

The nature of dispersion in the loss tangent ( $\tan \delta$ ) observed in oil shale is typically as shown in Fig. 10, which depicts the frequency-dependent loss tangent for a 26 gpt sample. The presence of a broad peak at low frequencies ( $< 100$  Hz) is interpreted in terms of interfacial polarization effects. The occurrence of secondary maxima in  $\tan \delta$  at higher frequencies, which is observed only at high temperatures, is also significant. The peak of these maxima shows a pronounced dependence on temperature, shifting to higher frequencies with increasing temperature. It is possible to extract activation energies for dipole relaxation processes from such temperature-dependent behavior. In materials as heterogeneous and complex as oil shale, the wide range of relaxation times significantly complicates the interpretation of these data. The dependence of the magnitude of  $\tan \delta$  on temperature also indicates that at high temperatures, where  $\tan \delta$  attains values greater than unity, the conduction is primarily ohmic, whereas at low temperatures where  $\tan \delta < 1$ , the conduction is by displacement current mechanisms. This behavior is consistent with the observed changes in the resistivity of oil shale as a function of temperature; decreases in the resistivity over five orders of magnitude are commonly observed for oil shale samples heated from room temperature to 450°C.

Figure 11 shows the loss tangent versus frequency for a 29.8 gpt shale. The same major features are observed as were observed for the 26 gpt sample. A secondary peak in the loss tangent appears at the temperatures where organic decomposition begins

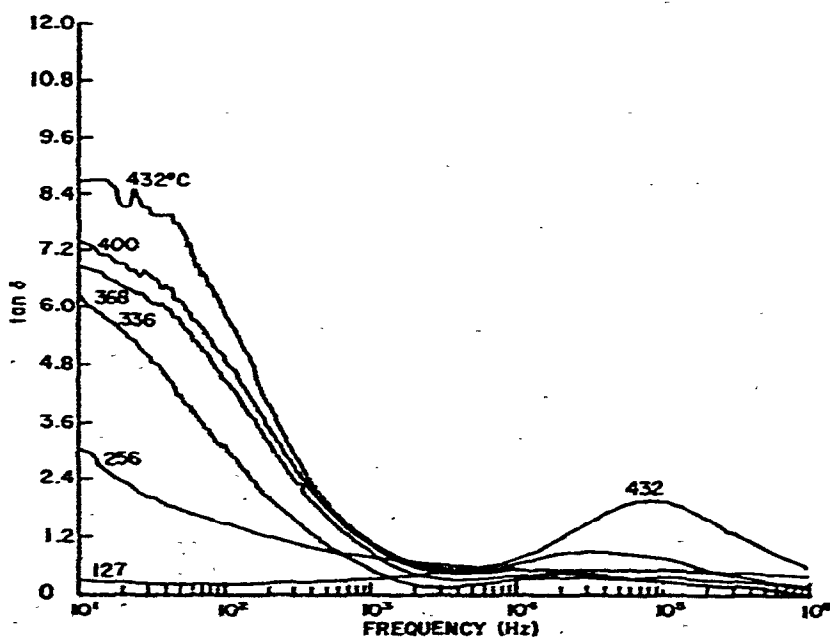


Fig. 11. Temperature-dependent loss-tangent versus frequency for a 29.8 gallons/ton oil shale.

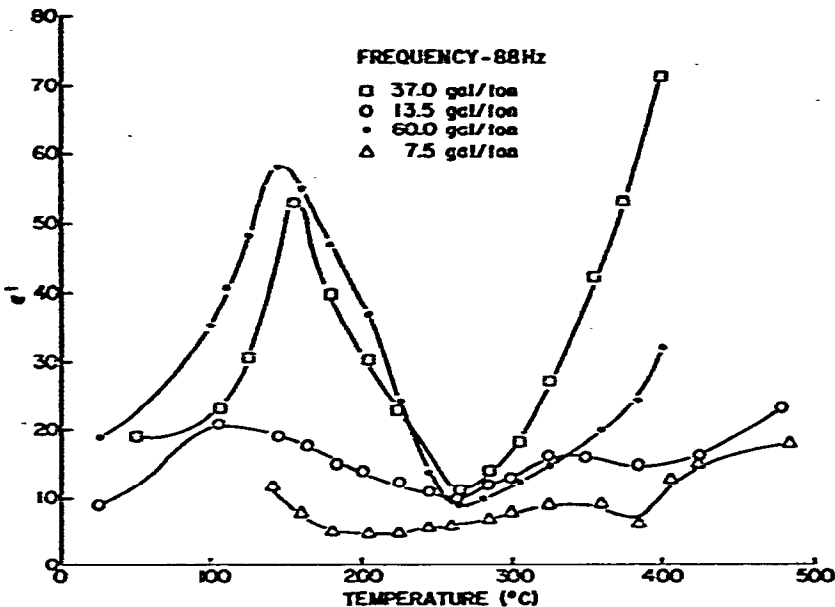


Fig. 12. Low-frequency dielectric constant versus temperature for various grades of oil shale.

to occur as indicated by the DTA curve. However, the temperatures at which this secondary peak begins to occur is lower on the higher grade of shale.

Figure 12 shows the temperature dependence of the dielectric constant of oil shale for different grades ranging from 7.5 to 60 gpt. The sharp changes in the  $\epsilon'$  values at temperatures in the range 100–150°C are correlated with the loss of capillary water and changes in the pore structure of the oil shale samples. The pronounced increase in the dielectric constant at temperatures above 270°C probably arises from the onset of the decomposition of the organic matter. The thermal behavior of the samples as shown by their DTA, which was carried out simultaneously with electrical impedance measurements, exhibits remarkably similar trends and points towards a common origin for the observed effects.

## CONCLUSIONS

The results indicate that interpretations based on a combined use of DTA and DA techniques yield valuable information for a complete characterization of thermo-physical behavior, especially for complex, heterogeneous materials like oil shale. The application of the technique of simultaneous DA–DTA to the study of polymorphic transformation in solid materials is also an interesting possibility. The abrupt changes in the dielectric parameters during a phase transformation are particularly amenable for study by DA–DTA; the information obtained therein, on the nature of the transformation, can be correlated with DTA data to gain a useful picture of the transformation mechanism. A detailed study of the transformations in minerals and polymeric materials utilizing DA–DTA is currently in progress.



## ACKNOWLEDGMENT

The authors gratefully acknowledge valuable discussions with Steve Knight of the Technical Equipment Corporation, Denver, Colorado.

This research program was carried out with financial support from NSF(RANN) Grant AER75-18650 and Laramie Energy Research Center, U.S. ERDA Grant E-(29-2)-3564.

## REFERENCES

- 1 H. H. Heady, *Am. Mineral.*, 37 (1952) 804.
- 2 V. D. Allred, *Q. Colo. Sch. Mines*, 59 (1964) 97.
- 3 A. Y. Herrell and C. Arnold, Jr., *Thermochim. Acta*, 17 (1976) 165.
- 4 J. W. Smith and D. R. Johnson, *172nd National Meeting, Am. Chem. Soc., Div. Fuel Chem. Prepr.*, 21 (1976) 25.
- 5 P. R. Tisot and W. L. R. Murphy, *Chem. Eng. Prog. Symp. Ser.*, 61 (1965) 25.
- 6 P. R. Tisot, personal communication, September 1976.
- 7 J. B. DuBow and R. N. Nottenburg, *Symposium on Oil Shale, Tar Sands and Related Materials: Preprints of Papers*, 1976, p. 77.
- 8 K. Rajeshwar, R. N. Nottenburg, J. B. DuBow and R. Rosenvold, *Thermochim. Acta*, in press.
- 9 J. W. Smith, in *Thermal Analysis, Proc. 3rd ICTA, Davos, 1971*, Vol. 3, Birkhauser Verlag, Basel, 1972, p. 605.
- 10 M. Weltner, *Acta Chim. Hung. Tomus*, 43 (1965) 89.
- 11 C. W. Beck, *Am. Mineral.*, 35 (1950) 985.
- 12 R. M. Gruver, *J. Am. Ceram. Soc.*, 33 (1950) 96.
- 13 J. L. Kulp, P. Kent and P. F. Kerr, *Am. Mineral.*, 37 (1952) 166.
- 14 J. W. Smith and D. R. Johnson, in H. G. McAdie (Ed.), *Proceedings of the Second Symposium on Thermal Analysis, Toronto*, Chem. Inst. of Canada, 1967, p. 96.
- 15 J. W. Smith and D. R. Johnson, *Amer. Lab.*, 3 (1971) 8.
- 16 J. DuBow (Ed.), *Electrical and Thermal Properties of Oil Shale of Interest to In-Situ Oil Extraction, Annual Report NSF RANN, AER 75-18650*, 1976.
- 17 P. D. Garn, *Thermoanalytical Methods of Investigation*, Academic Press, London and New York, 1965, p. 127.
- 18 J. W. Smith, *LERC/RI-76/6*, September 1976.
- 19 D. R. Johnson, N. B. Young and W. A. Robb, *Fuel*, 54 (1975) 249.
- 20 T. L. Webb and J. E. Kruger, in R. D. Mackenzie (Ed.), *Differential Thermal Analysis*, Vol. I, Academic Press, London and New York, 1970, p. 308.
- 21 E. I. Parkhomenko, *Electrical Properties of Rocks*, Plenum Press, New York, 1967, Chapter IV, p. 200.
- 22 R. H. Cole, in *Progress in Dielectrics*, Vol. 3, Wiley, New York, 1961, pp. 47-100.
- 23 G. V. Keller and P. H. Licastro, *Geog. Survey Bull.*, 1052-H, 1959.